



HAL
open science

Modified diffusion model adapted to non-unity Lewis number mixtures for low flame stretch using the thickened flame model

Sandy Poncet, Cedric Mehl, Karine Truffin, Olivier Colin

► To cite this version:

Sandy Poncet, Cedric Mehl, Karine Truffin, Olivier Colin. Modified diffusion model adapted to non-unity Lewis number mixtures for low flame stretch using the thickened flame model. 11th European Combustion Meeting - ECM 2023, Combustion Institute - French Section, Apr 2023, Rouen, France. hal-04112105

HAL Id: hal-04112105

<https://ifp.hal.science/hal-04112105>

Submitted on 31 May 2023

HAL is a multi-disciplinary open access archive for the deposit and dissemination of scientific research documents, whether they are published or not. The documents may come from teaching and research institutions in France or abroad, or from public or private research centers.

L'archive ouverte pluridisciplinaire **HAL**, est destinée au dépôt et à la diffusion de documents scientifiques de niveau recherche, publiés ou non, émanant des établissements d'enseignement et de recherche français ou étrangers, des laboratoires publics ou privés.

Modified diffusion model adapted to non-unity Lewis number mixtures for low flame stretch using the thickened flame model

S. Poncet^{*1}, C. Mehl¹, K. Truffin¹, and O. Colin¹

¹IFP Energies Nouvelles, Institut Carnot IFPEN Transports Energie, 1-4 Avenue du Bois-Préau, 92500 Rueil-Malmaison, France

Abstract

This study proposes a methodology based on species diffusion adaptation to recover flame response to stretch in the context of the Thickened Flame Model for non-unity Lewis mixtures. First, the flame speed variation induced by low stretch, that is overestimated by the standard form of the TFM, is illustrated with stoichiometric C₈H₁₈/air ($Le > 1$) and lean H₂/air ($Le < 1$) stretched thickened flame fronts. Secondly, the model correction parameter is deduced from spherical flame simulations for both mixture conditions. *A posteriori* validations, performed on spherical flames and flame-vortex interaction configurations, finally illustrate the effectiveness of this method. Keywords: Stretch, Diffusion, Non-unity Lewis number, Laminar premixed flame, Thickened Flame Model

Introduction

In Large Eddy Simulations (LES) of reactive flows, the flame thickness is usually small compared to the mesh size ($\Delta x \gg \delta_L^0$). The Thickened Flame Model (TFM), consisting in the artificial widening of the flame front, is a competitive approach which ensures the proper resolution of flame fronts [1], while preserving the correct propagation speed.

In TFM with full species and transport resolution, chemistry is solved using Arrhenius laws allowing for various phenomena such as flame-wall interactions, ignition and flame stabilization to be predicted accurately [2, 3]. However, a flame front thickened by a factor F is F times more sensitive to stretch than a real flame [2]. Various studies [4–6] proposed a tabulated adaptation of the species diffusion coefficients to account for strain effect of turbulent flows for CH₄/air mixtures ($Le \sim 1$). With a similar approach, Comer *et al.* [7] adapted the TFM approach in the context of strain-induced extinction limits for lean C₃H₈/air mixtures ($Le > 1$). Those studies only consider counter-flow strained flame configurations to determine their model correction parameters. Quillatre [8] proposed a diffusion-correction to limit the error of flame response to low stretch with TFM for non-unity Lewis mixtures based on asymptotic theories. However, restrictive assumptions of asymptotic theories didn't allow for the accurate preservation of flame speed for stretched-flame configurations.

The aim of this study is to propose a model to recover the flame response to low stretch in the context of the TFM approach for non-unity Lewis number mixtures. Unlike previous studies [4–7], we propose to address both strain and curvature effects by considering curved flames configurations. In Sec 1, we briefly recall the theory of the stretch influence on flame speed and the impact of the TFM on stretched flame configurations. In Sec 2, we develop a methodology, based on

the modification of species diffusivities, to correct the over-sensitivity of thickened flame fronts to stretch. The newly introduced method is assessed for a lean H₂/air ($Le < 1$) and a stoichiometric C₈H₁₈/air ($Le > 1$) mixtures. *A posteriori* validations are finally performed in Sec. 3 on spherical flames and flame-vortex interactions.

1 Theoretical background

1.1 Premixed flame stretch sensitivity

The balance between thermal energy released by oxidation reactions and the supply of chemical energy from reactive species, sustaining the combustion process in premixed flames, can be altered by flame stretching. Stretch is defined as the rate of change of the surface A normalised by its area and is evaluated as $K = 1/A \times dA/dt$. Under the assumptions of the asymptotic theory, the flame speed exhibits a linear trend that scales with stretch [9]. The flame speed is linearly dependant on stretch when either considering the *flame consumption speed* S_c or the *flame displacement speed* S_d^0 considered close to the burnt gas side [10]. On the one hand, the flame consumption speed represents the speed at which the flame consumes the reactants such as:

$$S_c = -\frac{1}{\rho_u (Y_{k_u} - Y_{k_b})} \int_{x^-}^{x^+} \dot{\omega}_k dn \quad (1)$$

where ρ , Y_k , $\dot{\omega}_k$ and n are respectively the density, the mass fraction of species k , the reaction rate of species k and the distance along the flame normal. x^- and x^+ represent the coordinates in the unburnt and burnt gas side of the reactive front. Indexes u and b refer to the unburnt and burnt gases, respectively. On the other hand, the flame displacement speed S_d^b corresponds to the velocity of an iso-surface of the flame considered in the burnt gas.

The impact of stretch on flame speed is characterized by the Markstein length L . Giannakopoulos *et al.* [10] distinguish the consumption Markstein length L_c and the

^{*}Corresponding author: sandy.poncet@ifpen.fr
Proceedings of the European Combustion Meeting 2023

displacement Markstein length L_d^b .

$$S_c = S_L^0 - L_c K \quad (2)$$

$$\widehat{S}_d^b = S_L^0 - L_d^b K \quad (3)$$

where \widehat{S}_d^b is the normalized displacement speed defined by $\widehat{S}_d^b = \sigma^{-1} S_d^b$ with the expansion ratio $\sigma = \rho_u/\rho_b$. The difference $L_d^b - L_c$ is always positive (see Eq. (34) in [10]), i.e. $L_d^b > L_c$, implying that these Markstein lengths can have opposite signs.

1.2 Stretch sensitivity of thickened flames

Based on the asymptotic theory, the consumption Markstein length scales with the flame thickness as $L_c \propto \delta_L^0 (Le_i - 1)$, where Le_i is the Lewis number of the limiting reactant of the mixture and is defined as the ratio between thermal diffusivity α and mass diffusivity of species D_i . Hence, for mixtures with large disparities between species mass diffusion and thermal diffusion, i.e. Le_i far from unity, the flame speed is significantly modified by stretch. As a consequence, with TFM, L_c is proportional to the thickened flame thickness, $F \delta_L^0$ where F is the thickening factor. A modification of the original TFM model is then necessary to account for stretch effects in flames modeled with preferential diffusion. Quillatre [8] proposed a corrected Lewis number Le_k^* for all species k based on the conservation of L_c , estimated from the asymptotic theory:

$$Le_k^* = 1 + \frac{Le_k - 1}{F} \Leftrightarrow Sc_k^* = Pr + \frac{Sc_k - Pr}{F} \quad (4)$$

This model was shown to reduce the over-estimation of the stretch effect with TFM [8]. However, the asymptotic theory being only qualitative for real multi-species chemistries, this approach still leads to important errors. Therefore, we propose here a model based on flame simulations which allows to accurately recover the real Markstein length of the flame.

2 TFM with corrected stretch sensitivity

2.1 Model formulation

Following previous approaches [7, 8] we propose to modify species diffusivities to correct the flame response to stretch. We define effective diffusion coefficients D_k^* , and thus Lewis numbers Le_k^* , as follows:

$$D_k^* = \frac{D_k}{\gamma} \quad \text{or} \quad Le_k^* = \frac{\alpha}{D_k^*} = \gamma Le_k \quad (5)$$

where γ is a model parameter determined so that the flame sensitivity to stretch is correctly retrieved. γ is *a priori* dependent on the local thermo-chemical conditions (pressure, temperature, equivalence ratio,...) and the thickening factor F . The modification of the diffusive fluxes however leads to an alteration of the flame speed and thickness. To recover the unstretched laminar flame speed, the pre-exponential factors of all reaction

rates are multiplied by a parameter A . It is evaluated as the ratio $A = (S_L^0/S_L^\gamma)^2$, with S_L^γ the flame speed obtained by using the effective diffusivity D_k^* without correcting the pre-exponential factor.

2.2 Model parameter evaluation

The method to estimate the model parameter γ is now described. In practice, we want to find the value of γ for each thickening factor F , written γ^F , which satisfies:

$$L(F, \gamma^F) = L(F = 1, \gamma = 1) \quad (6)$$

where L denotes here either the consumption or displacement Markstein length. We consider the Markstein number Ma defined as:

$$Ma(\gamma) = \frac{L(F, \gamma)}{F \delta_L^0} \quad (7)$$

Dividing Eq. (6) by $F \delta_L^0$ leads to the following identity:

$$Ma(\gamma = \gamma^F) = \frac{Ma(\gamma = 1)}{F} \quad (8)$$

The methodology adopted to determine γ^F is then as follows: (i) we compute a series of stretched flames with varying values of γ , using each time the adequate correction factor $A(\gamma)$, and we record the Markstein number $Ma(\gamma)$. These flames may be computed at any fixed thickening F by virtue of the proportionality relationship given in Eq. (7). (ii) We solve Eq. (8) for the unknown variable γ^F using an adequate optimization algorithm. The procedure is illustrated in Fig. 1. Step (i) might be performed by considering either curved or strained flames. In the present paper, the estimation of γ^F is performed by considering spherical curved flames. A more detailed discussion of this choice is left for future work. Additionally, γ_F might be determined considering the consumption or the displacement Markstein, leading to different estimations. A discussion on this aspect will be given in Sec. 3.

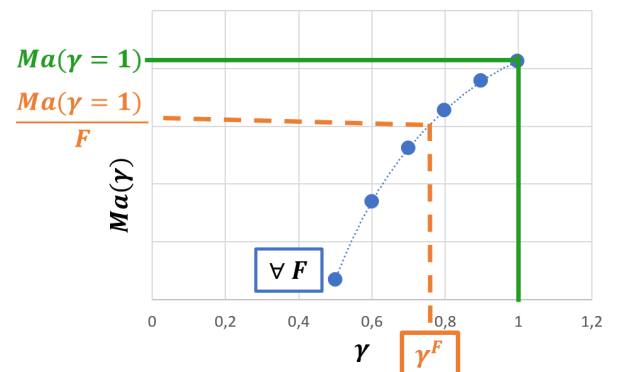


Figure 1: Illustration of the method to determine γ^F

2.3 Validation conditions

The proposed methodology is assessed on stoichiometric C_8H_{18}/air ($Le > 1$) and lean H_2/air ($Le < 1$)

mixtures. Both mixtures are considered at temperature $T = 300K$ and pressure $P = 1bar$. A 2-step mechanism involving 6 species [11] is used for the iso-octane case while a detailed mechanism (21 reactions, 10 species) [12] is used for the lean hydrogen mixture ($\Phi = 0.47$). The laminar flame characteristics, obtained from premixed adiabatic laminar flames computed with the CANTERA 1D solver [13], are (i) $S_L^0 = 0.35m/s$ and $\delta_L^0 = 357\mu m$ for the C_8H_{18} case (ii) $S_L^0 = 0.41m/s$ and $\delta_L^0 = 466\mu m$ for the H_2 case.

3 Results and discussion

The application of the corrected TFM model to H_2 and C_8H_{18} cases is explored here. It is first applied on spherical flames in Sec. 3.1, which serve both to fit the γ parameter and as a first validation set-up. The model is then validated on flame-vortex interactions in Sec. 3.2.

3.1 Spherical flames

3.1.1 Numerical set-up

Spherical-flame simulations are performed with the CONVERGE CFD software [14], which features a finite volume solver on Cartesian meshes. The present work considers in particular the resolution of 1-D spherical flame equations. This formulation enables an efficient computation of these flames and avoids the presence of intrinsic 3-D flame instabilities. The simulation domain length a is scaled with the thickening factor F such that $a = F \times 0.73m$ for both mixture cases. Mesh size is set as $\Delta_x = F \times (\delta_L^0/10)$. Hence, for every thickening factor considered, the flame front is solved on approximately $n \sim 10$ grid points.

3.1.2 Markstein lengths for spherical flames

We consider a spherical flame front propagating in the outwards direction into quiescent premixed fresh gases. The rate of change of the flame surface is directly related to the flame radius R_{BG} , determined in the burnt gas side:

$$K = \frac{2}{R_{BG}} \frac{dR_{BG}}{dt} = \kappa S_d^b \quad (9)$$

S_d^b and κ represent respectively the flame front displacement speed and the flame front curvature considered in the burnt gas. The flame front radius is evaluated from the burnt gas mass in the computational domain. The flame displacement speed considered in the burnt gas side is $S_d^b = dR_{BG}/dt$.

The consumption and displacement Markstein lengths are determined by a linear regression of $S_c(K)$ and $\widehat{S}_d^b(K)$ on the stretch rate interval $K = [20/F; 100/F]s^{-1}$. Figure 2 shows the displacement and consumption Markstein numbers as a function of γ for the H_2 case.

Table 1 provides values of the Markstein lengths, for thickening factors values equal to 1 and 8. It emphasizes

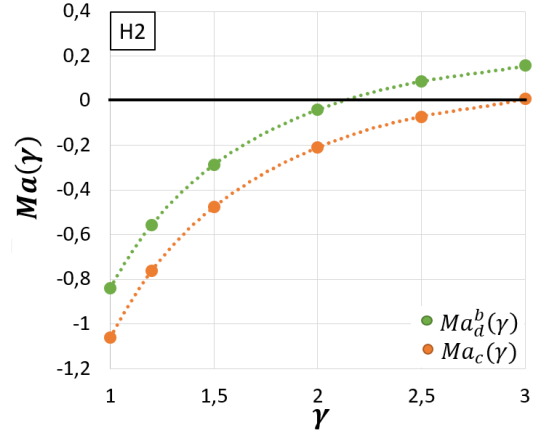


Figure 2: Markstein numbers with respect to γ for H_2 mixture ($\Phi = 0.47, T = 300K, P = 1bar$)

in particular the impact of thickening factor F on Markstein lengths, with $L(F = 8) \sim 8L(F = 1)$ regardless of the definition selected for L .

Table 1: Markstein lengths evaluated from the linear regression of flame consumption speed S_c (Eq2) and flame displacement speed \widehat{S}_d^b (Eq3)

Fuel	Variable	F=1	F=8	$L(F = 8)$
				$L(F = 1)$
C8H18	$L_d^b(1, F)$	0.099	0.768	7.8
	$L_c(1, F)$	0.070	0.540	7.7
	$L_d^b - L_c$	0.029	0.228	7.9
H2	$L_d^b(1, F)$	-0.399	-3.126	7.8
	$L_c(1, F)$	-0.503	-3.960	7.9
	$L_d^b - L_c$	0.104	0.834	8.0

3.1.3 Estimation of γ^F

The methodology presented in Sec. 2 is used to determine the appropriate γ^F to retrieve the reference Markstein length for a thickened flame. In particular, the evolution of $Ma(\gamma)$ computed from spherical flames, as represented in Fig. 2 for the H_2 case, is used to determine γ^F . Table 2 gives the correction factor values γ^F for various thickening factors F , based either on $Ma_d^b(\gamma)$ or $Ma_c(\gamma)$.

Table 2: Correction factor values γ^F based on Ma_c and Ma_d^b .

Fuel	Method	$\gamma^{F=4}$	$\gamma^{F=8}$	$\gamma^{F=16}$
		C8H18	displacement	0.545
	consumption	0.622	0.589	0.574
H2	displacement	1.621	1.829	1.959
	consumption	1.860	2.211	2.472

3.1.4 A posteriori validation on spherical flames

Fig. 3 illustrates the evolution of S_c with the stretch K for the H_2 spherical flames. The reference case is represented by the continuous black line. For the present

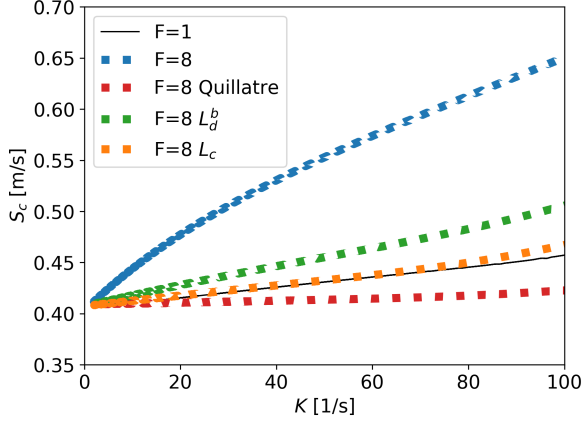


Figure 3: Flame consumption speed with respect to stretch for the H_2 mixture ($\Phi = 0.47, T = 300K, P = 1bar$)

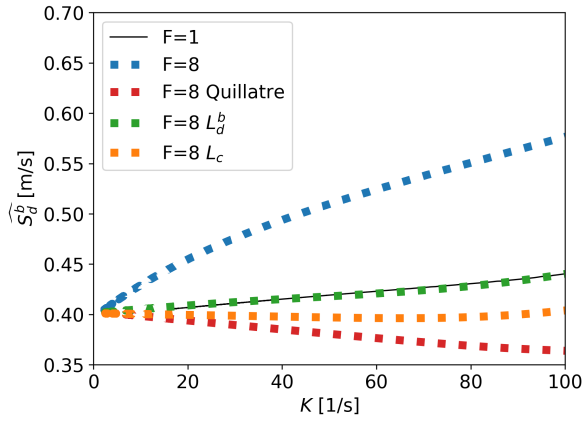


Figure 4: Flame displacement speed with respect to stretch for the H_2 mixture ($\Phi = 0.47, T = 300K, P = 1bar$)

lean H_2 /air mixture ($Le < 1$), the consumption Markstein length is negative and S_c is greatly overestimated for the $F = 8$ thickened flame. A simulation with the TFM correction proposed by Quillatre [8] is also added in Fig. 3. According to Eq. (4), the corrected Lewis numbers rapidly tends towards 1 as F increases. This is evidenced here in Fig. 3 by the fact that S_c computed with Quillatre's correction is insensitive to curvature. The flame consumption speed is overestimated when using $\gamma^{F=8}$ estimated from $Ma_d^b(\gamma)$, as seen in Figure 3. On the contrary, S_c is perfectly recovered when using $\gamma^{F=8}$ estimated from $Ma_c(\gamma)$. Similarly, stretched-flame displacement speeds $\hat{S}_d^b(K)$ obtained with those various approaches are provided with Fig. 4. The flame displacement speed is overestimated for the non-corrected thickened flame while it is underestimated with Quillatre correction and diffusion correction based on $Ma_c(\gamma)$. The evolution of $\hat{S}_d^b(K)$ is accurately recovered with the corrected TFM based on $Ma_d^b(\gamma)$.

Finally, the proposed corrected TFM enables to recover an accurate flame response to stretch, either preserving the flame consumption speed or the flame displacement speed of an iso-surface considered in the burnt

gas. However, it appears that preserving both consumption Markstein lengths L_c and L_d^b is impossible. It is then necessary to understand which formulation performs better in actual flame-turbulence interactions. A first answer to this question is attempted in the next section, where flame/vortex interactions are considered.

3.2 Validation on flame-vortex interactions

3.2.1 Numerical set-up

The validation set-up consists of a planar flame propagating towards a vortex. The 2D computational domain is square with $l = 200\delta_L^0$ side length. The incoming vortex is defined with radius $R = 10\delta_L^0$ and its azimuthal velocity at R is $u' = 5S_L^0$. Hence, the characteristic vortex time is $\tau_{vortex} = R/u' = 2\tau_{flame}$, where $\tau_{flame} = \delta_L^0/S_L^0$ is the flame time. The base mesh size is such that the vortex radius is discretized on 12 grid points, i.e. $\Delta x = R/12 = 0.8\delta_L^0$, and the TFM-AMR model is used to ensure a flame front resolution of $n = 10$ points in the flame using Adaptive Mesh Refinement (AMR) [15]. Four simulations are carried out to evaluate the performance of the newly developed corrected TFM model: (i) a reference simulation with $F = 1$; (ii) a simulation with $F = 4$ and the standard TFM; (iii) a simulation with $F = 4$ and the corrected TFM based on L_d^b ; (iv) a simulation with $F = 4$ and the corrected TFM based on L_c . The initial vortex position is adjusted so that the centre of the vortex is equidistant from the peak reaction location for the real and thickened flame cases. We consider here the C_8H_{18} case only, since planar lean H_2 /air flames are subject to thermo-diffusive flame instabilities due to the low Lewis number. Hence, the methodology can't be assessed on the lean H_2 case because small-scale instability structures are nearly suppressed at $F = 4$ while they will appear at $F = 1$.

3.2.2 Results

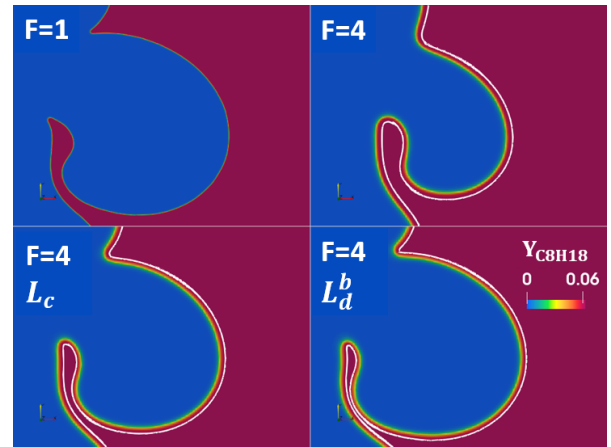


Figure 5: C_8H_{18} mass fraction profiles at $t = 17\tau_{flame}$ with ($F = 1; \gamma = 1$) (top left), ($F = 4; \gamma = 1$) (top right), ($F = 4; \gamma = 0.622$) (bottom left) and ($F = 4; \gamma = 0.545$) (bottom right). The white line represents the $T = 400K$ isotherm.

Fig. 5 shows the fuel mass fraction field for various configurations. The white line localizes the isotherm $T = 400K$. The reference case ($F = 1$) is a fully resolved non-thickened flame front. Results using the standard TFM model for $F = 4$ is represented on the top right plot. A clear difference of flame front surface is observed between the $F = 1$ and $F = 4$ cases. The concave region towards burnt gases enters deeper into the fresh gases for the reference flame than for the thickened flame. In fact, local flame speed is underestimated since Markstein length is overestimated by a factor $F = 4$ in the thickened case. Using diffusion corrections based on L_c and L_d^b , respectively on the bottom left and right in Fig. 5, the surface of the thickened flame is well retrieved.

A more quantitative comparison is performed considering space averaged properties of the flame. We define the flame length as:

$$L_{flame} = \int_S \|\nabla c\| dS \quad (10)$$

Where c is the progress variable defined as $c = 1 - Y_{C_8H_{18}}/Y_{C_8H_{18}}^u$, where $Y_{C_8H_{18}}^u$ corresponds to the value in fresh gases. S refers to the 2-D computational domain. The evolution of L_{flame} in time is represented in

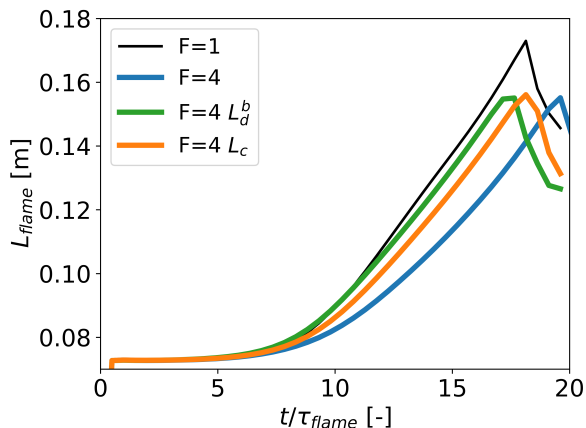


Figure 6: Flame length with respect to flame times.

Fig. 6. It shows a significant under-estimation of the flame length for the thickened case with standard TFM compared to the non-thickened case. This is due to the flame speed underestimation induced by TFM. For all thickened flame fronts, with or without the corrected diffusion coefficients, the maximal flame length is the same. The underestimation of the flame length maximum value for thickened flames compared to the reference flame is due to a loss of flame surface for highly curved zone encountered after the penetration of the vortex in the flame (see the snapshots in Fig. 5). For the thickened flame front without correction, the maximal flame length is reached with a delay equivalent to $1.5\tau_{flame}$ compared to the reference case (Fig. 6). On the contrary, the corrected TFM case based on displacement Markstein numbers reaches the maximal peak of

flame length with an advance of $0.5\tau_{flame}$. The maximal flame length is obtained simultaneously for the real flame and the thickened front with diffusion correction based on consumption Markstein numbers.

For a given flame geometry, here estimated by the flame length L_{flame} , an averaged flame consumption can be defined as:

$$\bar{S}_c = \frac{1}{L_{flame}} \times \frac{-1}{\rho_u (Y_{f_u} - Y_{f_b})} \int_S \dot{\omega}_f dS \quad (11)$$

with index f referring to the fuel species.

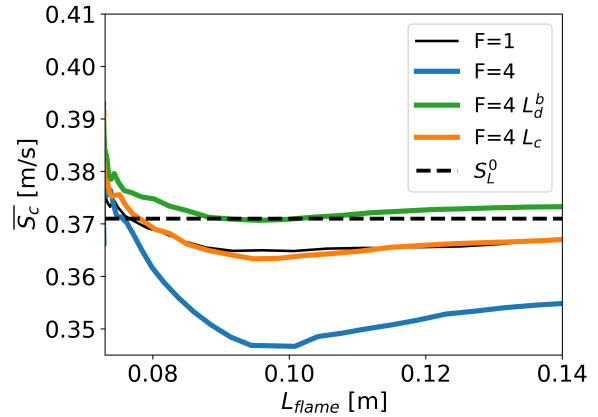


Figure 7: Averaged consumption speed with respect to the flame length.

Fig. 7 displays the averaged consumption speed as a function of the flame length. The laminar flame speed deduced from the simulation of a 1D planar flame with the CONVERGE solver [14], which equals $S_L^0 = 0.37m/s$ is added to the plot. The flame-vortex interaction induces a flame length increase with a predominantly concave curvature towards the burnt gases. As $Le > 1$, this configuration leads to a decrease of the flame speed as illustrated by the reference case in Fig. 7. The thickened flame front without correction features an overestimated decrease of the averaged speed, in line with the over-sensitivity of the TFM model to stretch. The averaged consumption speed obtained with the correction based on the displacement Markstein length is on the contrary over-estimated which is consistent with conclusions drawn from Fig. 3. For the thickened flame front with diffusion correction deduced from the consumption speed, \bar{S}_c coincides with the reference case. Hence, the change of consumption speed induced by preferential diffusion effects is accurately recovered for a thickened flame front when modifying species diffusion according to the proposed methodology performed with the consumption Markstein number Ma_c .

Conclusions

The present study proposes a framework to correctly take into account stretch effects on artificially thickened flames. The standard TFM approach induces an over-sensitivity of thickened flame fronts to stretch, which leads to a multiplication of the Markstein length by the

thickening factor F . To overcome this limitation, we proposed a TFM-adapted methodology to recover the flame speed of weakly stretched flames. The model, based on the adaptation of species Lewis numbers, was evaluated both for a $Le < 1$ mixture (lean H_2 /air case) and for a $Le > 1$ mixture (stoichiometric C_8H_{18} /air case). The present work illustrates the distinction between the influence of stretch (i) on flame consumption speed and (ii) on flame displacement speed, characterized respectively by a consumption Markstein length L_c and a displacement Markstein length L_d^b [10]. It was shown that our TFM-adapted diffusion model can be used either to recover the reference value of L_c or L_d^b . However, it is not possible to preserve both Markstein lengths simultaneously. Both approaches were shown to provide improved results compared to the standard TFM on a flame-vortex interaction case. Choosing L_c as a target allows in addition to recover nearly exactly the mean consumption speed. Both approaches will need to be evaluated on practical burner cases in a future study.

Acknowledgements

The authors gratefully acknowledge Damien Aubagnac-Karkar (IFPEN) for his technical and scientific assistance on the implementation of the model in the Cantera software.

References

- [1] T. D. Butler and P. J. O'Rourke, A numerical method for two dimensional unsteady reacting flows, *Symposium (International) on Combustion* **16**, 1503 (1977), ISSN 00820784.
- [2] D. Veynante and T. Poinso, instabilities in turbulent premixed burners large eddy simulation of combustion instabilities in turbulent premixed burners, *Center for Turbulence Research* (1997).
- [3] O. Colin and M. Rudgyard, Development of high-order taylor–galerkin schemes for les, *Journal of Computational Physics* **162**, 338 (2000), ISSN 00219991.
- [4] F. Proch and A. M. Kempf, Modeling heat loss effects in the large eddy simulation of a model gas turbine combustor with premixed flamelet generated manifolds, *Proceedings of the Combustion Institute* **35**, 3337 (2015), ISSN 15407489.
- [5] W. Han, H. Wang, G. Kuenne, E. R. Hawkes, J. H. Chen, J. Janicka, and C. Hasse, Large eddy simulation/dynamic thickened flame modeling of a high karlovitz number turbulent premixed jet flame, *Proceedings of the Combustion Institute* **37**, 2555 (2019), ISSN 15407489.
- [6] S. Popp, G. Kuenne, J. Janicka, and C. Hasse, An extended artificial thickening approach for strained premixed flames, *Combustion and Flame* **206**, 252 (2019), ISSN 00102180.
- [7] A. L. Comer, T. P. Gallagher, K. Duraisamy, and B. A. Rankin, A modified thickened flame model for simulating extinction, *Combustion Theory and Modelling* **26**, 1262 (2022), ISSN 1364-7830.
- [8] P. Quillatre, Ph.D. thesis, Université de Toulouse (2014).
- [9] M. Matalon and B. J. Matkowsky, Flames as gas-dynamic discontinuities, *Journal of Fluid Mechanics* **124**, 239 (1982), ISSN 0022-1120.
- [10] G. K. Giannakopoulos, C. E. Frouzakis, S. Mohan, A. G. Tomboulides, and M. Matalon, Consumption and displacement speeds of stretched premixed flames - theory and simulations, *Combustion and Flame* **208**, 164 (2019), ISSN 00102180.
- [11] E. Suillaud, K. Truffin, O. Colin, and D. Veynante, Direct numerical simulations of high karlovitz number premixed flames for the analysis and modeling of the displacement speed, *Combustion and Flame* **236**, 111770 (2022), ISSN 00102180.
- [12] M. Ó Conaire, H. J. Curran, J. M. Simmie, W. J. Pitz, and C. K. Westbrook, A comprehensive modeling study of hydrogen oxidation: A Comprehensive Modeling Study of Hydrogen Oxidation, *International Journal of Chemical Kinetics* **36**, 603 (2004), ISSN 05388066.
- [13] D. G. Goodwin, H. K. Moffat, I. Schoegl, R. L. Speth, and B. W. Weber, Cantera: An object-oriented software toolkit for chemical kinetics, thermodynamics, and transport processes, <https://www.cantera.org> (2022), version 2.6.0.
- [14] K. J. Richards, P. K. Senecal, and E. Pomraning, CONVERGE 3.0 (2022).
- [15] C. Mehl, S. Liu, and O. Colin, A strategy to couple thickened flame model and adaptive mesh refinement for the les of turbulent premixed combustion, *Flow, Turbulence and Combustion* **107**, 1003 (2021), ISSN 1386-6184.